



Simultaneous Design of a Small UAV (Unmanned Aerial Vehicle) Flight Control System and Lateral State Space Model

Sezer ÇOBAN^{1*}, Tuğrul OKTAY²

¹ College of Aviation, Iskenderun Technical University, Iskenderun, Turkey

² Department of Aeronautical Engineering, Erciyes University, Kayseri, Turkey

Abstract

In this study, the design of a small unmanned aerial vehicle (UAV) and the real-time application of the flight control system and lateral state-space model were investigated. For this purpose, an UAV production was carried out, which was assembled from different locations at certain intervals to the wing and tail set body and moved back and forth before the flight. An autopilot was then used which allowed the change of P, I, D values between 1 and 100. First of all, we obtained a lateral state space model of the UAV and obtained a simulation model of Unmanned Aerial Vehicle. At the same time, the block diagram of the autopilot system was extracted and modeled in MATLAB / Simulink environment. Afterwards, SPSA developed a cost function consisting of ascent, seating time and maximum overrun, and the Unmanned Aircraft and autopilot system were redesigned simultaneously to minimize this cost function. High performance is easily observed in simulation responses and real flights.

Keywords: Simultaneous design, Autonomous performance

1. Introduction

The UAV, which we produce to improve the flight performance, is produced using simultaneous unmanned aerial vehicle and autopilot system design. The ailerons on the UAV wings have a direction rudder connected to the vertical stabilizer and the vertical rudder due to the horizontal stabilizer.

However, the UAV has an engine that will provide the energy of a propeller and propeller system used to produce propulsion. Various sensor packages, which are the auxiliary elements of our autopilot system, are available in our UAV.

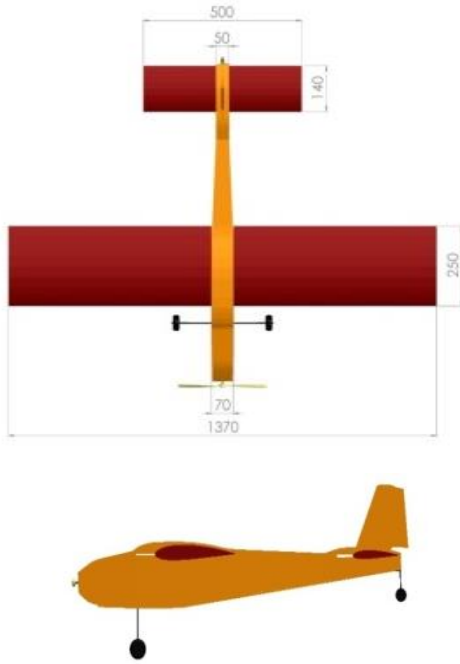


Figure 1. Wing Motion Mechanisms of UAV

In order to perform any dynamic modeling of any aircraft or any UAV, the equations of the aircraft body must first be obtained. These equations can be classified into three groups. These equations are the force equations of the body, the moment equations and kinematic equations. Newton's second law was used in the literature to extract the force equations. Equation (1) provides this law:

$${}^I \vec{F} = M_a \frac{d\vec{V}_{cg}}{dt} = M_a \left[\frac{\partial \vec{V}_{cg}}{\partial t} + {}^I \vec{\omega} \otimes \vec{V}_{cg} \right] \quad (1)$$

The components of the force on three axes (x, y, z) are expressed in terms of the weight of the aircraft, linear accelerations ($\dot{u}, \dot{v}, \dot{w}$), linear velocities (u, v, w), angular velocities (p, q, r) and Euler orientation angles (ϕ_A, θ_A) [1,2].

State and control variables of the linearized model in Table 1 are summarized. As seen, the state vector has 9 variables and the control vector has 4 variables.

Compared to the general approach mentioned above, dynamic modeling of fixed-wing aircraft has been widely used in the literature. In fixed-wing aircraft, there is very little relationship between

longitudinal movement dynamics and lateral movement dynamics and this relationship is negligible. In addition, the movement of the vertical axis has little effect on aircraft dynamics [3,4]. Therefore, longitudinal and lateral movement can be examined independently of each other.

Table 1. State and Control Variables of Linearized Models

Durum Değişkeni	Nicelik	Kontrol Değişkeni	Nicelik
x_1	u	u_1	δ_e
x_2	v	u_2	δ_T
x_3	w	u_3	δ_a
x_4	p	u_4	δ_r
x_5	q		
x_6	r		
x_7	ϕ_A		
x_8	θ_A		
x_9	ψ_A		

2. State Space Model, Controller And SPSA Optimization Method

In Equation (2) the Lateral State Space Model of our UAV is given:

$$\begin{bmatrix} \Delta \dot{v} \\ \Delta \dot{p} \\ \Delta \dot{r} \\ \Delta \dot{\Phi} \end{bmatrix} = \begin{bmatrix} Y_v & Y_p & -(u_0 - Y_r) & g \cos \theta_0 \\ L_v & L_p & L_r & 0 \\ N_v & N_p & N_r & 0 \\ 0 & 1 & 0 & 0 \end{bmatrix} \begin{bmatrix} \Delta v \\ \Delta p \\ \Delta r \\ \Delta \Phi \end{bmatrix} + \begin{bmatrix} 0 & Y_{\delta_r} \\ N_{\delta_a} & L_{\delta_r} \\ N_{\delta_a} & N_{\delta_r} \\ 0 & 0 \end{bmatrix} \begin{bmatrix} \Delta \delta_a \\ \Delta \delta_r \end{bmatrix} \quad (2)$$

Our P-I-D based autopilot system is shown in Figure 2. Six P-I-D controllers were used to control the distance between the designated distances.

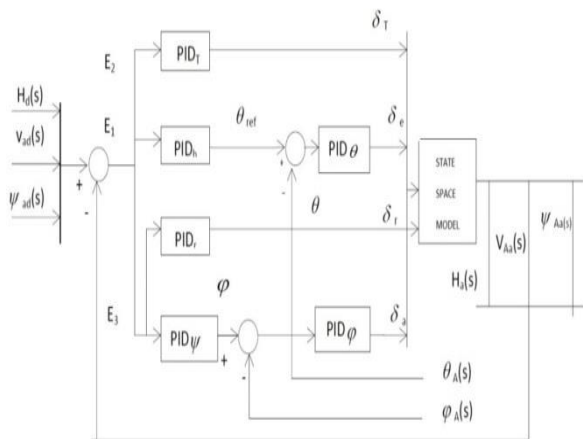


Figure 2. Hierarchical Detailed Autopilot Structure of the UAV

Aerodynamic forces acting on an UAV body placed experimentally in the wind tunnel can be obtained with a force measurement system. However, it is quite costly to make the calculation of these forces by examining each body shape in a separate wind tunnel. In addition, it is not possible to calculate analytically due to the nonlinear complex components contained in the aerodynamic forces. For this reason, stochastic estimation methods are used.

Simultaneous Perturbation Stochastic Approximation (SPSA) is one of the methods based on random estimation [5]. In many studies, it has been shown that SPSA provides better results compared to optimization algorithms such as genetic and heat treatment, which have higher computational costs than SPSA [6]. In addition, SPSA provides very successful results for limited optimization problems. Another feature of SPSA is that it contains a natural randomness because it is an estimation method. Thus, SPSA can find the best solution in a few steps without being attached to a specific local point [7].

We used an adjustable autopilot using flight observations and our autopilot system has a classic autopilot structure. There are three layers for the

hierarchical control structure and are divided into outer loop, middle loop and inner loop which was showed in figure 3 .

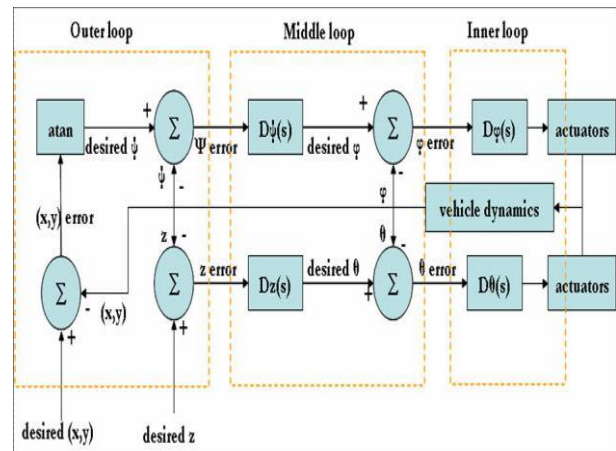


Figure 3. Control Structure of Autopilot System

3. Structural Analysis of The UAV

ANSYS finite software elements were used in structural analysis of UAV. The analyzes were performed by a 16-processor workstation with a speed of 2.5 Ghz and 32 GB of RAM.

For modeling, 20 mesh 3D elements were used and experimental conditions were determined as much as possible. Figure 3 shows the deviation of the UAV on the wing. The deviation increases as the wings reach the tip and reaches the highest value when the end of the wing is reached. Figure 4 shows the Von Mises stress values on the wing of the UAV. Von Mises stress values change according to the change in bending resistance across the canteen. As a result, the largest Von Mises stress value is found at the root of the wing. The best place for carbon tubes is where the voltage produced by the foam and carbon tubes is below the maximum voltage value.

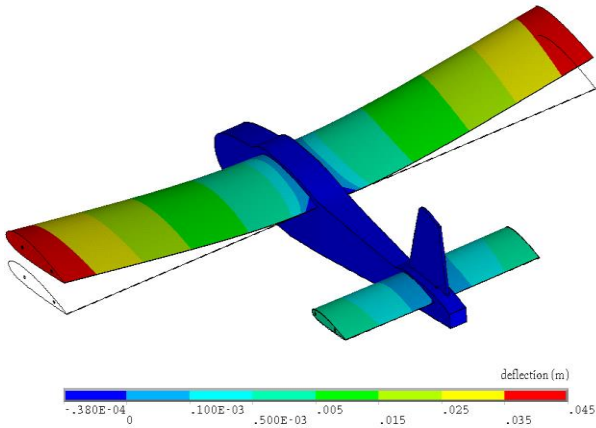


Figure 3. Deviation Results of the UAV (For a Velocity of 60 km / h)

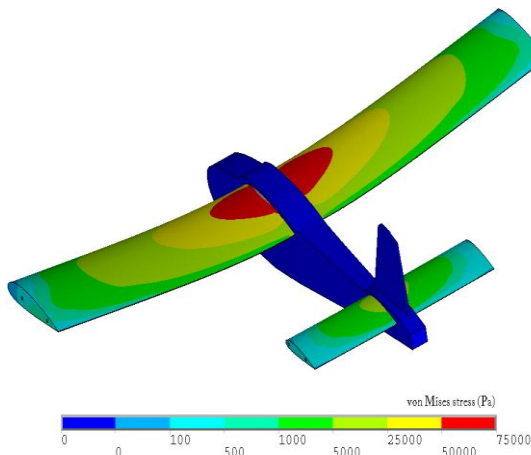


Figure 4. Von Mises Stress Results (60 km / h) [12]

4. Results

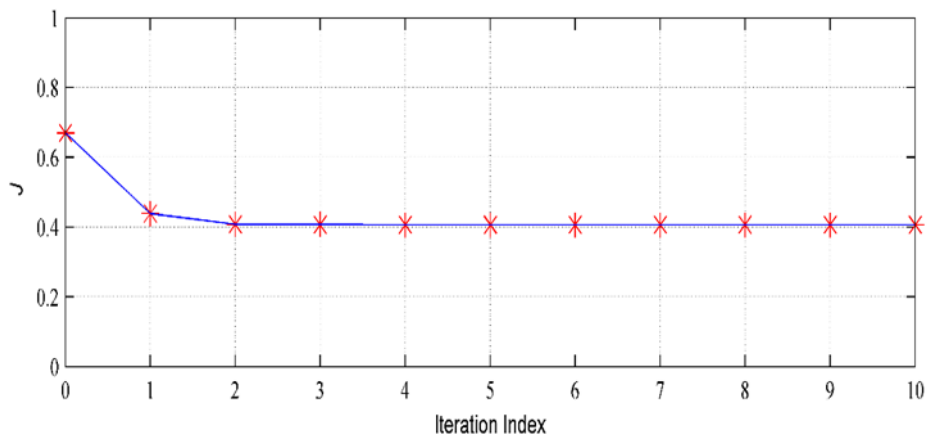
Simulation results of lateral movement are presented as a result of simultaneous design using SPSA optimization method. Minimization of cost function, relative energy saving and final trajectory

tracking results are given. In turbulent environment, trajectory monitoring and closed loop responses of the control surface (Aileron) are presented.

In the example examined in this study, the problem was simplified and only converted to a sub-sample related to rolling control. The optimization variables for this problem are the gain parameters of the respective PID controller of the wing and tail assembly mounting positions of the casing and the bearing angle. The trajectory monitored is a 5-degree rolling angle signal in the form of a unit-step. The control surface that provides this is aileron. Turbulence environment is also taken into account and there is also a 1 degree saturation function on the aileron control surface. The results obtained during the simultaneous design were found and also the closed loop responses were obtained in the presence of atmospheric turbulence [13].

In Figure 5, minimization of cost function, relative energy saving and final trajectory tracking results are given. In Figure 6, closed loop responses of trajectory monitoring and other state variables and control surface (Aileron) are presented in turbulent environment.

As a result of the simultaneous design, significant improvement (approx. 40%) was obtained in the autonomous performance index, which consisted of sitting time, rise time, and maximum excess. This ratio is about 40%, and is obtained from the relative relationship between the value obtained before the concurrent design and the result obtained from the concurrent calculation.



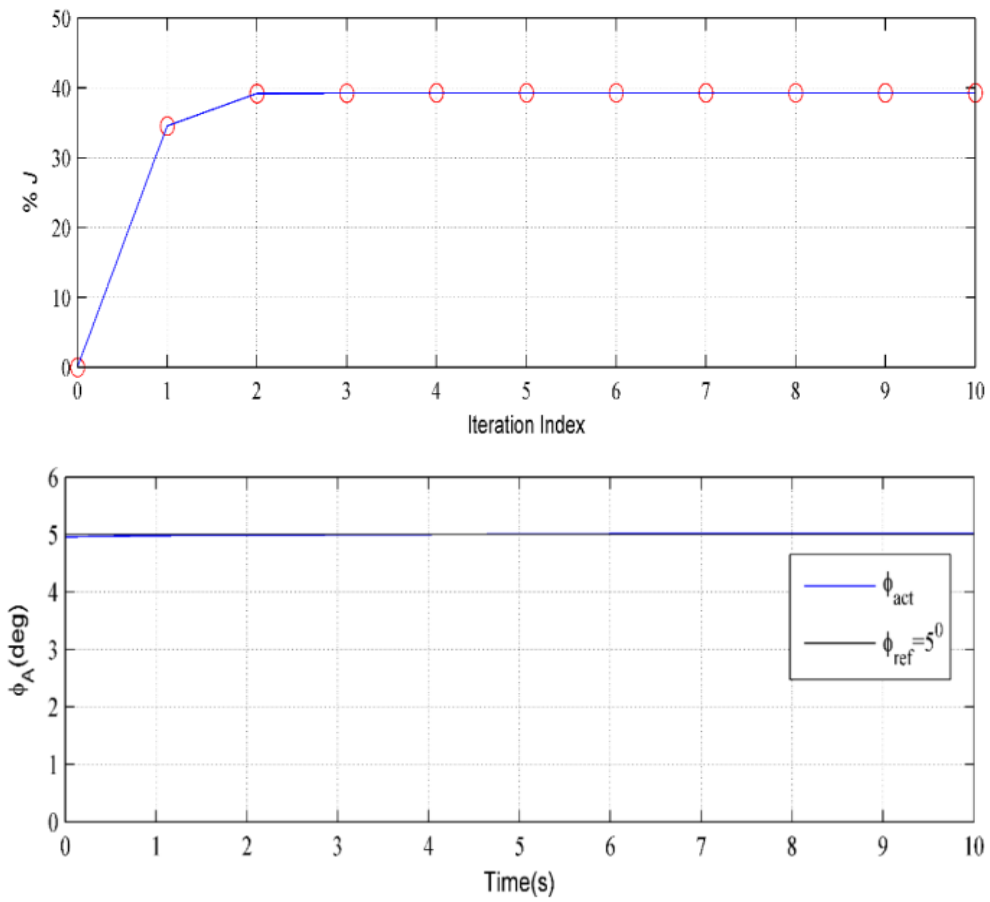
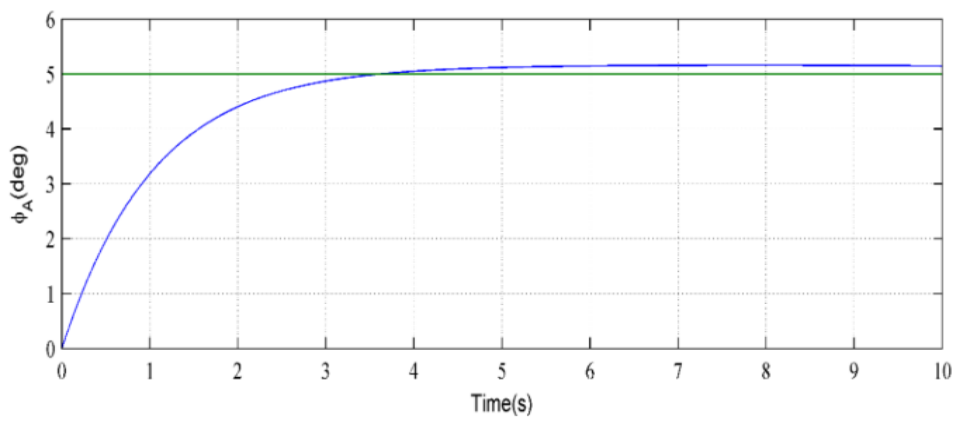


Figure 5. Cost Minimization, Relative Energy Saving and Orbit Tracking



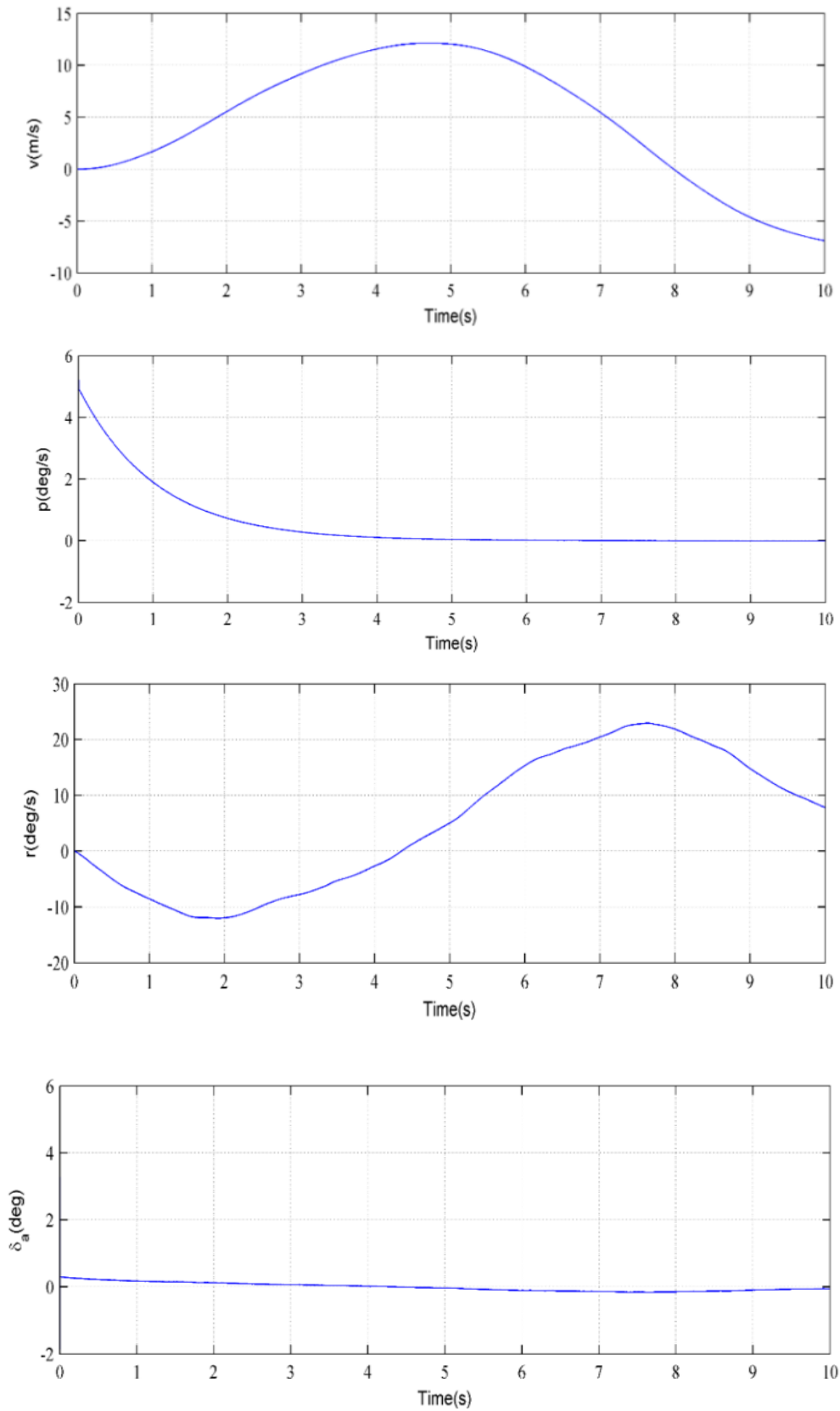


Figure 6. Orbital Tracking and Other State Variables in Closed Turbulent Environment and Closed Cycle Responses of Control Surface

Significant autonomous performance improvement was achieved with very small changes in UAV geometry. As a result of the simultaneous design method implemented and developed within the scope of the study, autonomous performance has been improved significantly. Furthermore, even in the simulation environment where turbulence exists, success in trajectory tracking has been achieved. This method is also applicable in different UAVs.

References

- [1] Nelson, R. C. (1998). Flight stability and automatic control (Vol. 2). WCB/ McGraw Hill.
- [2] Greenwood, D. T. (2003). Advanced Dynamics, Cambridge University Press. ISBN 0-521-82612-8.
- [3] Padfield, G. D. (2007). Helicopter Flight Dynamics, AIAA Education Series.
- [4] Etkin, B., & Reid, L. D. (1996). Dynamics of flight: stability and control (Vol. 3). New York: Wiley.
- [5] Oktay, T., Konar, M., Mohamed, M. A., Aydin, M., Sal, F., Onay, M., & Soylak, M. Autonomous Flight Performance Improvement of Load-Carrying Unmanned Aerial Vehicles by Active Morphing. World Academy of Science, Engineering and Technology, International Journal of Mechanical, Aerospace, Industrial, Mechatronic and Manufacturing Engineering, 10(1), 123-132, 2016.
- [6] Spall, J. C., (1992) "Multivariate stochastic approximation using a simultaneous perturbation gradient approximation," IEEE Trans. Autom. Control, 37 (3), 332–341.
- [7] Maryak, J. L., & Chin, D. C. (2001). Global random optimization by simultaneous perturbation stochastic approximation. In American Control Conference, 2001. Proceedings of the 2001, 2:756-762.
- [8] Wang, I. J., & Spall, J. C. (2003, December). Stochastic optimization with inequality constraints using simultaneous perturbations and penalty functions. In Decision and Control, 2003. Proceedings. 42nd IEEE Conference on (Vol. 4, pp. 3808-3813). IEEE.
- [9] He, Y., Fu, M. C., Marcus, S. I., (2003) "Convergence of Simultaneous Perturbation Stochastic Approximation for Non-Differentiable Optimization", IEEE Transactions on Aerospace and Electronic Systems, 48 (8):1459–1463.
- [10] Kuo, B. C. (1963). Analysis and synthesis of sampled-data control systems. Prentice-Hall
- [11] Ekinci, İ (2016). İnsansız Bir Hava Aracının Yanal Durum Uzay Modelinin ve Uçuş Kontrol Sisteminin Eş Zamanlı Tasarımı. Erciyes Üniversitesi Fen Bilimleri Enstitüsü, Yayınlanmış Yüksek Lisans Tezi, Kayseri
- [12] Perkins, C. D., & Hage, R. E. (1949). Aircraft performance, stability and control. John Wiley
- [13] Oktay T., Çoban S. , "Simultaneous Longitudinal and Lateral Flight Control Systems Design For Both Passive and Active Morphing TUAUVs ", ELEKTRONİKA İR ELEKTROTEKNİKA, vol.23, no.5, pp.15-20, 2017